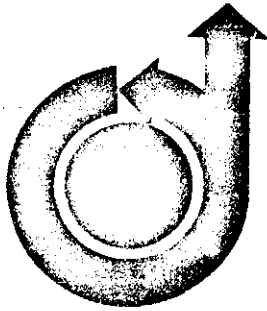


(AIAA - P - 77 - 520)



77-520

**High Power Spark Gap Switches- a
Numerical Model and Experimental
Investigations, *J. F. Driscoll and
R. E. Ponsonby, Univ. of Michigan,
Ann Arbor, Mich.,
and J. Heckl, Naval Weapons Center,
Silver Springs, Md.***

AIAA CONFERENCE ON THE FUTURE OF AEROSPACE POWER SYSTEMS

St. Louis, Missouri/March 1-3, 1977

For permission to copy or republish, contact the American Institute of Aeronautics and Astronautics,
1290 Avenue of the Americas, New York, N.Y. 10019.

M77-11947

HIGH POWER SPARK GAP SWITCHES — A NUMERICAL
MODEL AND EXPERIMENTAL INVESTIGATION

James F. Driscoll*
Ralph E. Ponsonby**
Department of Aerospace Engineering
The University of Michigan
Ann Arbor, Michigan

J. Heckl
and
Naval Surface Weapons Center
Silver Spring, Maryland

Abstract

A numerical model has been developed, and an experimental program undertaken to improve the operating characteristics of high power spark gap switches passing Megawatt average power, with hold-off voltages of several hundred kilovolts, and repetition rates above 100 pulses per second. The model and measurements are being used to understand and predict the effects of various interrelated parameters, including gas flow rate and pressure, gap spacing and geometry, recovery voltage and current waveform, and pulse repetition frequency. The numerical model predicts the approximate dielectric recovery rate and the grace period required before subsequent switching. Photographic and spectroscopic measurements of arc properties are described.

I. Introduction

Present and future applications of Aerospace, shipboard and ground based pulsed power systems require closing switches that are more advanced than the present state of the art. High power switching devices play a vital role in power conditioning networks in properly adapting capacitive storage systems to meet the requirements of various loads. A high power spark gap switch program has been initiated to meet requirements of a triggered closing switch capable of several hundred pulses per second. Other switches also under consideration include Thyratrons, Liquid Metal Plasma Valve (LMPV) and Crossed Field closing switches. Design goals for the present program are given in Table I.

TABLE I. NSWC PROGRAM DESIGN GOALS
(Per Electrode Pair)

Average Power	2.5 - 5 MW
Holdoff Voltage	100 - 300 KV
Pulse Width	20 - 50 μ sec
Energy per Pulse	10 - 100 kiloJoules
Repetition Rate	50 - 250 pps
Recovery Rate	> 250 V/ μ sec
Lifetime	10^5 pulses
Efficiency	> 98 percent
Weight, Volume	Minimum

A numerical model has been developed and experimental measurements are being performed to understand and control the interaction between the arc discharge and the gas flow in a spark gap switch. Fundamental research performed at The University of Michigan, in conjunction with the Naval Surface Weapons Center, has been coordinated with a parallel effort involving design and fabrication of an improved spark

gap switch. Design and testing of the prototype switch is being performed by Maxwell Laboratories.

II. Related Research

Results of a previous program, conducted by the Air Force Aero Propulsion Laboratory (AFAPL) are directly applicable to the present study. The AFAPL switch was developed by Maxwell Laboratories, Inc.¹, and is shown schematically in Fig. 1. This spark gap switch consists of two inch diameter electrodes and is operated with overvoltage triggering. The electrodes are made of copper with elkonite (Tungsten-Silver) tips. Dry air flows radially inward at flow rates up to 150 cubic feet/minute (CFM) and is exhausted through the hollow copper electrodes. The gap spacing (2) of the electrodes is 0.5 cm.

The accomplishments per electrode pair for the AFAPL program are given in Table II

TABLE II. AFAPL ACCOMPLISHMENTS
(Per Electrode Pair†)

Average Power	1.4 MW
Holdoff Voltage	20 KV
Pulse Width	\approx 20 μ sec
Energy per Pulse	5.6 kiloJoules
Repetition Rate	100 - 500 pps
Gas Flow	150 CFM (Air)
Switch Grace Period	~ 700 μ sec
Charge Transfer	
per Pulse	280 mC
Lifetime	10^6
Efficiency	~ 99.7 percent
Weight	30 lbs
Volume	0.63 ft ³
Triggered	Overvolting Mode

†Two-inch OD electrodes made of copper with Tungsten-Silver tips.

The direction of gas flow as shown in Fig. 1 was found to be important; reversing the flow by introducing gas through the electrodes caused a much slower switch recovery. Reversed flow direction caused the arc discharge to be convected in a direction of decreasing flow velocity so that arc transit time through the gap was increased. When the gas is exhausted through the electrodes, arc velocity increases toward electrode centerline, and the hot gas is convected at high velocity out of the switch.

*Assistant Professor, Member AIAA.

**Member AIAA.

Results of the AFAPL switch tests indicate that the following twelve variables, listed in Table III, are important in high power spark gap switch operation.

TABLE III. PARAMETERS AFFECTING SWITCH OPERATION

Gas Flow Rate (ϕ)	Gap Spacing (λ)
Gas Type	Electrode Shape
Gas Pressure (P)	Electrode Material
Current Pulse [I(t)]	Grace Period
Operating Voltage (V)	Recharge Time
Charge Transfer (Q)	Repetition Frequency

The above parameters were found to be interrelated, complicating the optimization of switch performance. Gas velocity was found to be one of the most important parameters. Local velocity depends on flow rate, electrode geometry, gap spacing and gas pressure. Maximum pulse repetition frequency is a function of recharge rise-time, operating voltage, and grace period before application of voltage waveform.

The measured restrike rate was found to decrease if the gas velocity was increased. Increased restrike rate occurred due to increased charge transfer per shot, rate of rise of recharge voltage, and a decrease in grace period. Larger gap spacings actually increased restrike rate because flow velocity diminished. It was also found that by obtaining higher gas velocities by using smaller diameter electrodes, all other parameters being fixed, operation at higher voltages and lower flow rates was possible.

To hold off voltages of 300 Kv, high gas pressures and/or large gap spacings are required. For dry air, more than 5 atmospheres pressure are required for gap spacing of 2 cm. Both high gas pressure and the large gap spacing lead to high gas flow requirements. Increasing the gap spacing length necessitates increased gas flow in order to maintain a constant flow velocity in the gap region. As a result of these considerations, it can be seen that the design of a spark gap to be operated at high repetition frequencies and high voltage involves a careful balancing and optimization of several factors. A method currently considered² to increased holdoff voltage yet minimize gas flow rate is to operate several gas cooled spark gaps in series. Analysis shows this to be more practical than the increasing gap dimension λ because gas flow rate increases as λ^3 while holdoff voltage increases proportional to λ .

III. Numerical Model

During normal operation of a repetitive spark gap switch, energy is deposited in the spark channel by Joule heating during the conduction cycle. This energy is partially radiated away, partly conducted to the electrodes, and partly removed by convection. For the switch to function properly, it is necessary that the dielectric strength of the gas be restored after each

shot before voltage is reapplied. Otherwise, the switch will restrike prior to the next pulse. In order for the dielectric strength of the gas to be restored between shots, it is necessary to remove or cool the hot gas generated by the spark. The electrodes themselves are also cooled by the gas flow. Gas flow cooling is especially important in the operation of high power repetitious spark gaps.

A numerical model has been developed which predicts the dielectric strength of the flowing gas and the trends in restrike probability as switch parameters are varied. The gas flow pattern and all important heat transfer mechanisms have been included in the model. The discharge column length, radius, and temperature are determined as functions of time during the current pulse and subsequent gas cooling period.

The primary motivation for the model is to assess the effects of the interrelated switch parameters listed in Table III to optimize design tradeoffs. The numerical model has also been used to determine which experimental measurements are most useful to better understand switch performance.

The spark gap switch is modelled by two electrodes with geometry as shown in Fig. 1. Geometry and dimensions correspond to the AFAPL test switch described previously. Gap spacing is 0.5 cm, outside diameter is 5.08 cm. The simple two electrode overvolted spark gap results in relatively uniform electric fields, thus higher holdoff voltages than trigatron spark gaps. Air flows radially inward as shown, exiting along the electrode axis. The design is a good one from a gasdynamic standpoint in that the discharge length is forced to increase by a factor of 5.5 as it is convected downstream of the minimum gap yet flow velocity in this region remains constant to within 10%.

The spark-generated arc discharge is assumed to have cylindrical geometry for simplicity. The low density, highly viscous hot gas column is essentially impervious to the surrounding gas flow, since by continuity the small absolute density variations in the low density column results in a net mass inflow that is a negligible fraction of the mass flow of the surrounding gas. A uniform radial temperature profile is assumed for simplicity; this assumption is nearly realized by radiation dominated arcs³. Conditions of local thermodynamic equilibrium can be expected to prevail for the presently considered electric fields, gas pressure of one atmosphere and time scales of many microseconds⁴.

The discharge is convected radially inward as shown in Fig. 1; an arc velocity of 95% of the calculated average gas velocity at that radial location has been used. Photographs of transversely blown discharges in similar gaps were used to

estimate arc relative velocity^{5,6}. Measurement of discharge velocity in the present geometry is a major goal of the experimental part of this program.

The partial differential equations governing heat transfer have been simplified to the following:

$$\rho C_p \frac{dT}{dt} = \frac{I^2}{\sigma A^2} - \epsilon U - 4\pi \frac{kT}{A} \quad (1)$$

$$\frac{d}{dt} (\rho C_p T A \ell) = \frac{I^2}{\sigma A} \ell - U A \ell - Nu k T \pi \ell \quad (2)$$

$$Nu = .466 Re^{.615} \quad (3)$$

Equation (1) is the energy balance on the arc centerline. Centerline temperature T and area A are determined as functions of time t . The current pulse waveform $I(t)$ is supplied to calculate the Joule heating term. Total radiation losses $U(T)$ in watts/cm³ for high temperature air at one atmosphere have been calculated by Hermann and Shade⁷, ϵ is a factor greater than unity that includes reabsorbed radiation and is determined from the same reference. Density, ρ , heat capacity, C_p , thermal conductivity, k , and electrical conductivity, σ , of air vary with temperature according to Yos⁸. Radial conduction losses in the partial differential equation have been approximated by $-4\pi kT/A$ which would be exact for the case of a parabolic temperature profile. This assumption, proposed by Lowke⁹, considerably simplifies the analysis; his results for an axially blown arc show good agreement with experiment.

Equation (2) is the boundary condition that defines the arc area such that total energy balance is satisfied, similar to that used by Frost and Liebermann¹⁰. Forced convection losses from a cylinder in transverse flow are given by Eq. (3) for Nusselt number Nu . Reynolds number, Re , is the relative velocity, U_r , times arc diameter divided by free stream kinematic viscosity.

The variation of arc length, (ℓ), is important in the final cooling process and is determined from:

$$\frac{d\ell}{dt} = \frac{2\dot{V}}{\pi} \frac{\sqrt{d^2 - (\ell - H)^2}}{[D - \sqrt{d^2 - (\ell - H)^2} (H - \ell) \ell]} \quad (4)$$

where \dot{V} is the gas flow rate in CFM, D and d are defined in Fig. 1.

The simplifying assumptions described above have been included in the model because it was felt that attempts to solve the full partial differential equations would not readily allow the inclusion of all important physical processes, especially transverse convection and arc length variations. In the present simplified model, the following input can be varied: current waveform, electrode geometry, gas flow rate, real gas transport properties, recovery voltage waveform, discharge relative

velocity, and initial conditions of temperature and area. Experimental measurements of the latter three quantities are presently being performed.

Solutions to Eqs. (1)-(4) were obtained using Hamming's modified predictor-corrector scheme. The scheme is a stable fourth order integration procedure initiated by a Runge-Kutta technique; correct step size for each iteration is determined for maximum accuracy.

Experimental data and dimensions of the AFAPL spark gap switch as shown in Fig. 1 were used. Current waveforms used in the model duplicated experimentally measured waveforms. In two series of tests, peak currents were 2.3 and 15 Kiloamps with pulse durations of 32 μ sec and 88 μ sec, respectively.

Results for one typical spark gap firing are shown in Fig. 2. Joule heating causes rapid increases in arc temperature and diameter. Radiation losses are dominant immediately after the current pulse, until the arc temperature decreases below 10,000°K. Convective cooling and arc stretching then dominate as the hot gas continues to move downstream with the flow. The slight increase in arc radius at 16,000°K is due to a large local maximum in the curve of heat capacity of air versus temperature.

For successful switch operation, the gas density must increase to nearly ambient density before the voltage waveform is reapplied, or restrike will occur. The breakdown potential for the gap has been calculated using empirical data¹¹ obtained at high temperatures and fit to the Paschen breakdown relation:

$$V_{BD} = \frac{6.958 \times 10^4 \ell/T}{\ln(668,900 \ell/T)} \quad (5)$$

where ℓ is the column length and temperature T is inversely proportional to gas density. Gas ionization is negligible for the temperatures that exist by the time the voltage waveform is reapplied. Breakdown voltage is plotted in Fig. 3 for the temperature decay illustrated in Fig. 2. When the breakdown potential (V_{BD}) of the hot cylinder finally exceeds that of the minimum gap itself, the latter constant quality is plotted.

A reapplied voltage waveform (V) similar to that used in the switch tests of Ref. 1, is shown in Fig. 3. After a grace time of 500 μ sec, the voltage rises in a $(1 - \cos \omega t)$ waveform with an average rate of rise of 14 v/ μ sec. Restrike probability shown in Fig. 2 has been calculated using the best available empirical relation between restrike rate and the voltage difference $(V_{BD} - V)$ ¹². More accurate experimental measurements of restrike probability for the present geometry are presently being performed.

Numerical results have been obtained for gas flow rates corresponding to switch tests of Ref. 1, and are shown in Figs. 2-5. An increase in gas flow rate causes an increase in gas cooling and dielectric recovery, causing restrike rate to decrease. The numerical model predicts the same trends as were observed experimentally in the AFAPL tests of Ref. 1. Higher gas flow rates are correctly predicted to be necessary to obtain higher pulse repetition rates.

The model also indicates that the problem is not simply one of blowing hot gas from the gap. When the arc radius expands as in Fig. 2, significant heating of gas upstream of the gap may occur; this gas travels at velocities only one tenth that of gas downstream of the gap. Significant heating of the low velocity gas upstream of the gap can seriously degrade switch performance. Furthermore, the arc velocity may not scale as the gas velocity and may be significantly lower than gas velocity under certain conditions.

Results of the analytic program to date indicate that experimental measurements of arc relative velocity and switch restrike probability are needed to provide empirical input directly applicable to the present geometry. The numerical model has shown that several causes of switch restrike are possible. For example, infrequent initial breakdown centered upstream of the minimum gap can lead to excessively large dielectric recovery times and switch restrike.

IV. Experimental Measurements

An experimental program is presently underway to measure discharge diameter, temperature, and relative velocity, and switch restrike probability. The University of Michigan's Cascade Arc Facility, shown schematically in Fig. 6, has been used to obtain repeatable and controlled arc discharges in flowing gases.

Schlieren photographs of discharge diameter and location are being made at framing rates of 2×10^6 frames/sec using a Beckman-Whitley camera¹³.

Temperature measurements are being made using a unique computer controlled optical scanning system. Intensities of the spectral multiplets at 5679 Å and 4793 Å in the NII emission spark spectrum are measured using a rotating mirror and GCA McPherson 216.5 Polychromator. Complete radial temperature profiles in the discharge are deduced at time intervals of 50 μsec from the measured light intensity profiles, after properly subtracting background intensity profiles and performing an Abel inversion.

For a plasma (singly ionized nitrogen in this case) having a Maxwell Boltzmann distribution of electronic energy levels, E_i , local temperature can be deduced from

the measured ratio of volume emission coefficients ϵ_i/ϵ_j of two spectral multiplets from:

$$T = \frac{(E_i - E_j)/k}{\ln \frac{g_i A_i v_i \epsilon_j}{g_j A_j v_j \epsilon_i}} \quad (6)$$

Quantities A_i and g_i are transition probabilities and multiplicity factors, respectively, corresponding to multiplet frequencies ν_i, ν_j which were selected for optimum measurement sensitivity.

A typical temperature profile of a .2Ka axially blown circuit breaker arc is shown in Fig. 7. Digital temperature values can be obtained at sample intervals as small as 10 nanoseconds in this facility. Temperature measurements for the spark gap geometry are presently in progress.

V. Conclusions

A program has been initiated to investigate the interactions between arc discharges and gas flows that occur in high power, high repetition rate spark gap switches.

1. A numerical model has been developed which predicts the discharge temperature, radius and length, as well as approximate dielectric recovery rate of the gap versus time. Maximum repetition rate of the switch is then predicted.
2. The model includes the processes of transverse convective cooling, radiation losses, arc length variations, and internal conduction. The program requires the following to be supplied: gap geometry, current pulse waveform, voltage recovery waveform, and real gas transport properties. Analytical work indicates that the following empirical input is important: arc relative velocity, initial area and temperature immediately after breakdown, and restrike probability phenomena.
3. An experimental program is presently in progress to obtain the above mentioned empirical data. Spectroscopic and photographic measurements of arc temperature, radius, velocity and restrike probability are being made in The University of Michigan's Cascade Arc Facility.
4. The numerical model correctly predicts a decrease in restrike rate as gas flow rate increases, as has been measured experimentally¹. Decreasing the rate of rise of recovery voltage and increase switch grace time also decreases restrike rate, in agreement with experiments. Switch performance is presently being predicted for variable geometry and current waveform.

References

1. Clark, W., "High Power Spark Gap Switch Development," AFAPL, TR-75-41, (1975).
2. Markins, Dennis, Maxwell Laboratory, private communication.
3. Lowke, J.J., "Characteristics of Radiation Dominated Electric Arcs," J. Applied Phys., 41, 6, 2588 (1970).
4. Griem, H., Plasma Spectroscopy, McGraw Hill, (1964).
5. Mallairis, A., "Interaction Between Electric Arc Discharges and Cross Flow," ARL-64-216 (1964).
6. Thiene, P., "Convective Flexure of a Plasma Conductor," Phys. Fluids 6, 9, p. 1319 (1963).
7. Hermann, W. and Schade, E., JQSRT, 12, 9, 1257 (1972).
8. Yos, J.M., AVCO Technical Memo RAD TM 637 (1963).
9. Lowke, J.J., "Properties of Vertical Arcs Stabilized by Natural Convection," Phenomenon in Ionized Gases, 12, 144 (1975).
10. Frost, L. and Liebermann, R., Proc. IEEE, 59, 474 (1971).
11. Powell, C.W., Ryan, H.M., and Reynolds, A., "Breakdown Characteristics of Air at High Temperatures," Second International Conference on Gas Discharges, London, (1972).
12. Burdin, R.A. et al., "A Compact Low Inductance 1.5 Ma 60KJ Capacitor Spark Gap Module," Second International Conference on Gas Discharges, London, (1972).
13. Phillips, R.L. and Anderson, R., "Experimental Study of Axially Blown Electric Arcs," Univ. of Michigan Report 011116 (1975).

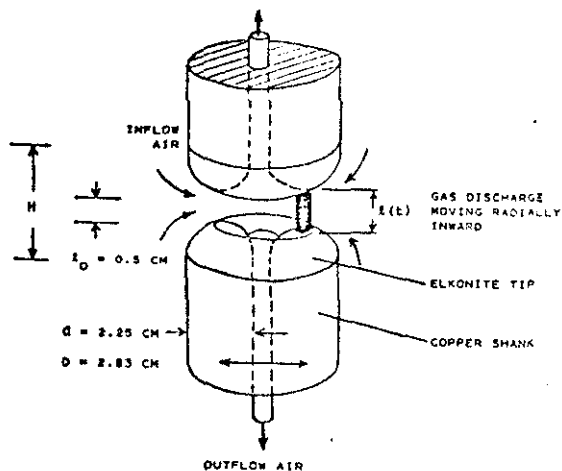


Figure 1. Schematic of High Power, High Repetition Rate Spark Gap Switch

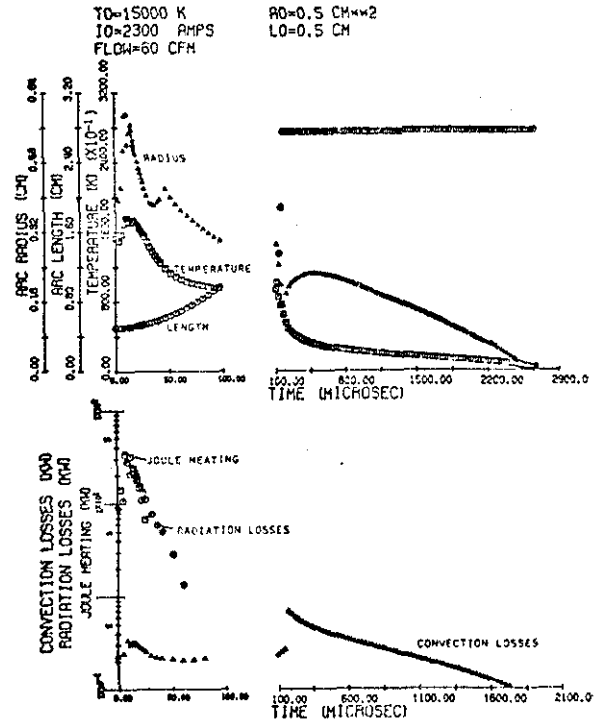


Figure 2. Calculated Arc Temperature, Radius, Length for 60 CFM Air Flow

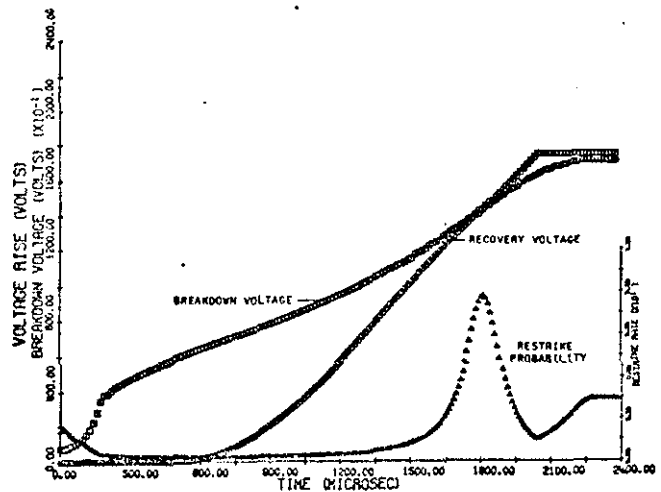


Figure 3. Breakdown, Recovery Voltages and Restrike Probability for 60 CFM Air Flow

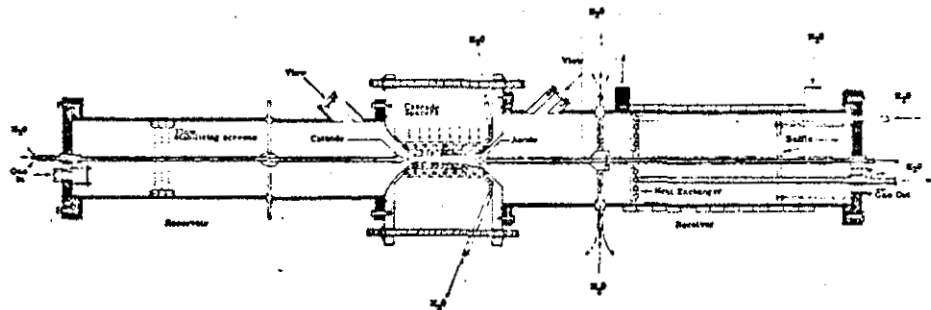


Figure 6. Schematic of the Cascade Arc Test Facility

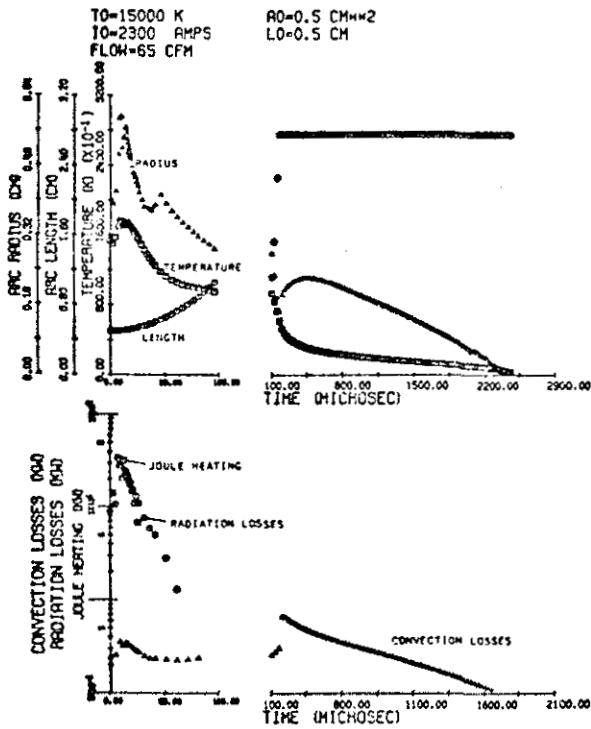


Figure 4. Calculated Arc Temperature, Radius, Length for 65 CFM Air Flow

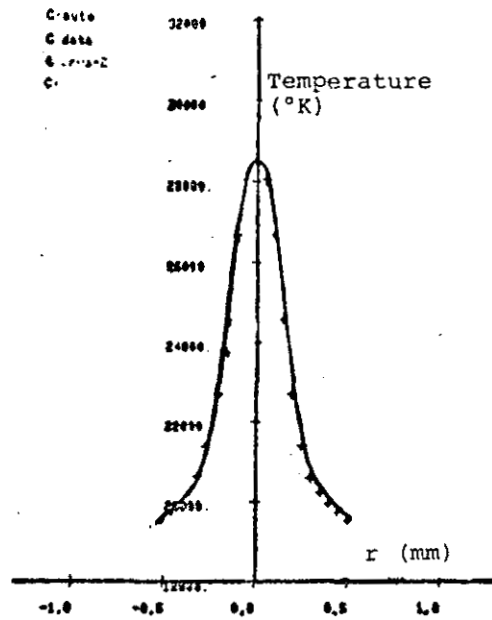


Figure 7. Spectroscopic Measurement of Arc Temperature Versus Radial Distance for an Axially Blown Arc

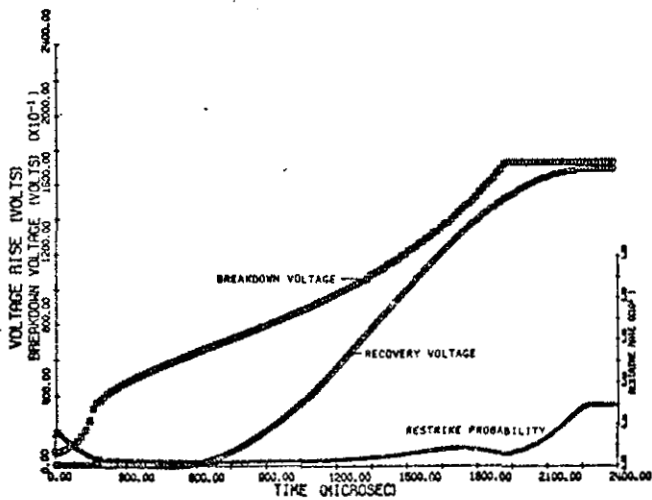


Figure 5. Breakdown, Recovery Voltages and Restrike Probability for 65 CFM Air Flow